ADVANCED MATERIALS

[3] M. A. Gondal, A. Hameed, Z. H. Yamani, A. Suwaiyan, *Chem. Phys. Lett.* **2004**, *385*, 111.
[4] a) X. N. Xu, Y. Wolfus, A. Shaulov, Y. Yeshurun, I. Felner, I. Nowik, Y. Koltypin, A. Gedanken, *Appl. Phys. Lett.* **2002**, *91*, 4611. b) W. Dong, C. Zhu, *J. Mater. Chem.* **2002**, *12*, 1676.
[5] J. Ji, S. Ohkoshi, K. Hashimoto, *Adv. Mater.* **2004**, *16*, 48.
[6] K. Woo, H. J. Lee, J. P. Ahn, Y. S. Park, *Adv. Mater.* **2003**, *20*, 1761.
[7] X. Wang, X. Chen, L. Gao, H. Zheng, M. Ji, C. Tang, T. Sen, Z. Zhang, *J. Mater. Chem.* **2004**, *14*, 905.
[8] Y. Y. Fu, R. M. Wang, J. Xu, J. Chen, Y. Yan, A. V. Narlikar, H. Zhang, *Chem. Phys. Lett.* **2003**, *379*, 373.
[9] X. P. Shen, H. J. Liu, L. Pan, K. M. Chen, J. M. Hong, Z. Xu, *Chem. Lett.* **2004**, *33*, 1128.
[10] Y. Xia, P. Yang, Y. Sun, Y. Wu, B. Mayers, B. Gates, F. Kim, H. Yan, *Adv. Mater.* **2003**, *15*, 353.
[11] P. M. Ajayan, *Chem. Rev.* **1999**, *99*, 1787.
[12] a) G. R. Patzke, F. Krumeich, R. Nesper, *Angew. Chem. Int. Ed.* **2002**, *41*, 2446. b) C. N. R. Rao, M. Nath, *Dalton Trans.* **2003**, 1. c) R. Tenne, *Angew. Chem. Int. Ed.* **2003**, *42*, 5124.
[13] a) M. Remskar, *Adv. Mater.* **2004**, *16*, 1497. b) D. Li, Y. Xia, *Adv. Mater.* **2004**, *16*, 1151.
[14] C. R. Martin, *Science* **1994**, *266*, 1961.
[15] M. Steinhart, J. H. Wendorff, A. Greiner, R. B. Wehrspohn, *Science* **2002**, *296*, 1997.
[16] E. D. Sone, E. R. Zubarev, S. I. Stupp, *Angew. Chem. Int. Ed.* **2002**, *41*, 1706.
[17] F. Schüth, *Angew. Chem. Int. Ed.* **2003**, *42*, 3604.
[18] M. Lahav, T. Sehayek, A. Vaskeich, I. Rubinstein, *Angew. Chem. Int. Ed.* **2003**, *42*, 5576.
[19] M. Steinhart, R. B. Wehrspohn, U. Gosele, J. H. Wendorff, *Angew. Chem. Int. Ed.* **2004**, *43*, 1334.
[20] K. Hara, N. Nishida, *Sens. Actuators, B* **1994**, *20*, 181.
[21] X. Q. Liu, S. W. Tao, Y. S. Shen, *Sens. Actuators, B* **1997**, *40*, 161.
[22] L. H. Luo, X. L. Li, W. Li, S. Q. Xi, *Sens. Actuators, B* **2000**, *71*, 77.
[23] M. Law, H. Kind, B. Messer, F. Kim, P. Yang, *Angew. Chem. Int. Ed.* **2002**, *41*, 2405.
[24] Y. Wang, X. Jiang, Y. Xia, *J. Am. Chem. Soc.* **2003**, *125*, 16 176.
[25] a) Y. Idota, T. Kubota, A. Matsufuji, Y. Maekawa, T. Miyasaka, *Science* **1997**, *276*, 1395. b) M. Winter, J. O. Besenhard, M. E. Spahr, P. Novak, *Adv. Mater.* **1998**, *10*, 725.
[26] J. M. Tarascon, M. Armand, *Nature* **2001**, *414*, 359.
[27] P. Poizot, S. Laruelle, S. Grugeon, L. Dupont, J. M. Tarascon, *Nature* **2000**, *407*, 496.
[28] D. Larcher, D. Bonnin, R. Cortes, I. Rivals, L. Personnaz, J. M. Tarascon, *J. Electrochem. Soc.* **2003**, *150*, A1643.
[29] S. Grugeon, S. Laruelle, R. Herrera-Urbina, L. Dupont, P. Poizot, J. M. Tarascona, *J. Electrochem. Soc.* **2002**, *149*, A285.
[30] D. Larcher, C. Masquelier, D. Bonnin, Y. Chabre, V. Masson, J. B. Leriche, J. M. Tarascon, *J. Electrochem. Soc.* **2003**, *150*, A133.
[31] a) F. S. Cai, G. Y. Zhang, J. Chen, H. K. Liu, S. X. Dou, *Angew. Chem. Int. Ed.* **2004**, *43*, 4212. b) J. Chen, Z. L. Tao, S. L. Li, *J. Am. Chem. Soc.* **2004**, *126*, 3060.
[32] Z. L. Tao, L. N. Xu, X. L. Gou, J. Chen, H. T. Yuan, *Chem. Commun.* **2004**, 2080.
[33] J. Chen, Z. L. Tao, S. L. Li, *Angew. Chem. Int. Ed.* **2003**, *42*, 2147.

Structural and Optical Properties of Uniform ZnO Nanosheets**

By *Shijian Chen*, *Yichun Liu*,* *Changlu Shao*, *Richard Mu*,* *Youming Lu*, *Jiying Zhang*, *Dezhen Shen*, and *Xiwu Fan*

Semiconductor nanostructures have attracted much attention as promising candidates for future electro-optical devices. In nanostructures, the carrier-state density is concentrated in discrete energy levels, which enables the enhancement of exciton oscillator strength and light-emitting efficiency. As a result, the performance of nanostructure-based optical devices is expected to be improved and be less temperature dependent.[1] Among the wide variety of semiconductor nanostructures, ZnO nanostructures, as wide bandgap semiconductors, are even more attractive for high-efficiency short-wavelength optoelectronic nanodevices,[2–4] due to their large excitonic binding energy (≈60 meV) and high mechanical and thermal stabilities. For one-dimensional ZnO nanostructures, different shape structures, such as tetrapod nanorods,[5,6] nanowires,[7,8] or nanobelts,[3,9] as well as their optical properties have been reported. Two-dimensional nanostructures, such as nanosheets, are another important category that have received increasing attention recently.[10–12] However, for ZnO, relatively few studies on two-dimensional (2D) nanostructures have been reported.[13,14] Nanostructured materials are expected to have improved optical properties compared with bulk materials. However, the reported photoluminescence (PL) spectra of ZnO nanostructures[14–17] have shown UV emission accompanied by strong deep-level (DL) emissions, which may be ascribed to many structural defects, such as stacking faults and dislocations, which exist in the nanostructures.[18] Since the performance of electronic and photonic devices is strongly dependent upon environmental conditions, such as temperature, humidity, etc., most optoelectronic devices fail to operate at high temperature. Hence, investigation of the high-temperature PL characteristics is important to explore the potential for future high-temperature nano-optoelectronic devices.

[*] Prof. Y. C. Liu, S. J. Chen, Dr. C. L. Shao
Centre for Advanced Optoelectronic Functional Material Research
Northeast Normal University, Changchun 130024 (PR China)
E-mail: ycliu@nenu.edu.cn
Prof. R. Mu
Department of Physics
Fisk University, Nashville, TN 37028 (USA)
E-mail: rmu@fisk.edu
Dr. Y. M. Lu, Dr. J. Y. Zhang, Dr. D. Z. Shen, Dr. X. W. Fan
Key Laboratory of Excited State Processes
Changchun Institute of Optics, Fine Mechanics and Physics
Chinese Academy of Sciences
16 East-South Lake Avenue, Changchun 130033 (PR China)

[**] This work was supported by the National Natural Science Foundation of China, No.60176003 and No.60376009, and the Foundational Excellent Researcher to Go Beyond the Century of the Ministry of Education of China. R. Mu acknowledges the financial support from ARO, NREL/DOE, and NSF-CREST of United States.

  DOI: 10.1002/adma.200401263

In this communication, we report the synthesis of micrometer-sized uniform ZnO nanosheets. The nanosheets have far superior high-temperature emission to any other materials that have been reported in the literature.

The morphology of the sample was characterized by field-emission scanning electron microscopy (FESEM). Typical examples are shown in Figures 1a,b. They are uniform multilayered sheets with lateral dimensions of several micrometers. Flat and smooth terraces and steps are clearly seen, which

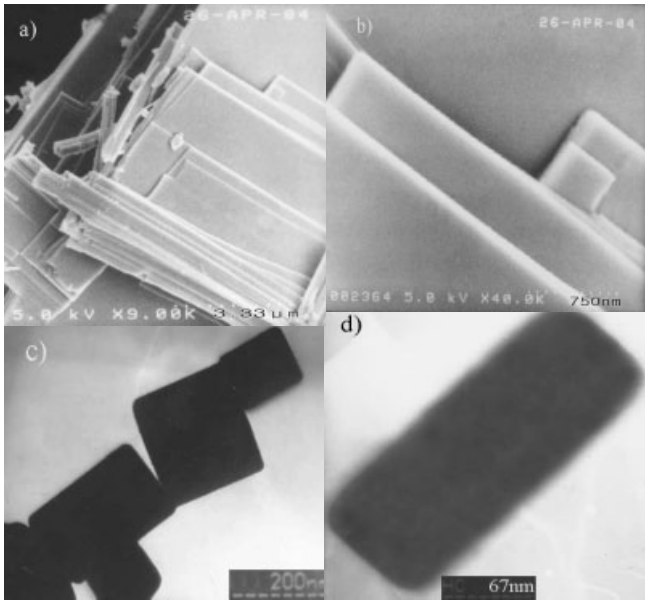

Figure 1. a) Low magnification FESEM image of ZnO nanosheets, b) higher magnification FESEM image indicating smaller sheets grown on the larger, c) low magnification TEM image of ZnO nanosheets showing block-like sheets, and d) higher magnification TEM image illustrating the rectangular cross-section of the sheets.

suggests a layer-by-layer growth mechanism. A smaller sheet can be seen lying on the larger one, indicating an initial phase of a sheet growth, as shown in Figure 1b. Cross-section transmission electron microscopy (TEM) measurements also show that some of the smaller samples are square and rectangular in shape and the size varies from 50 to 300 nm, as illustrated in Figures 1c,d. An X-ray diffraction (XRD) spectrum is displayed in Figure 2. The diffraction peaks fit well with a wurzite ZnO structure. No diffraction peaks are observed from metallic Zn. Electron back-scattered diffraction (EBSD) from the large sheets suggested that the sheets have a preferred $(2\bar{1}0)$ surface orientation.

Figure 3 shows a Raman spectrum of the ZnO nanosheets excited with an Ar ion laser at 488 nm. All observed spectroscopic peaks can be assigned to a wurzite ZnO structure according to the literature values,[19,20] which are listed in the inset of Figure 3.

Figure 4 represents three PL spectra measured at temperatures of 80, 300, and 857 K, respectively. The PL spectrum at

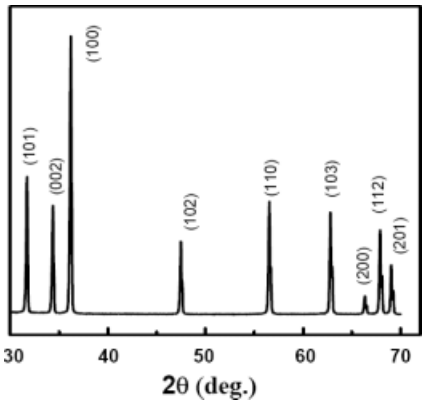

Figure 2. X-ray diffraction spectrum of the ZnO nanosheet structures.

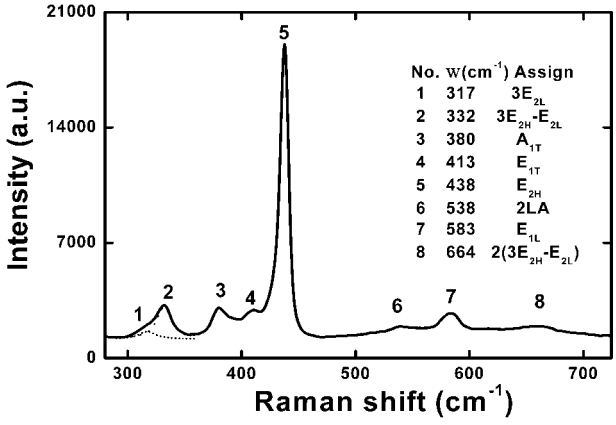

Figure 3. Raman spectra of ZnO nanosheets excited at 488 nm. Inset table shows the Raman frequencies and assignments of all the peaks.

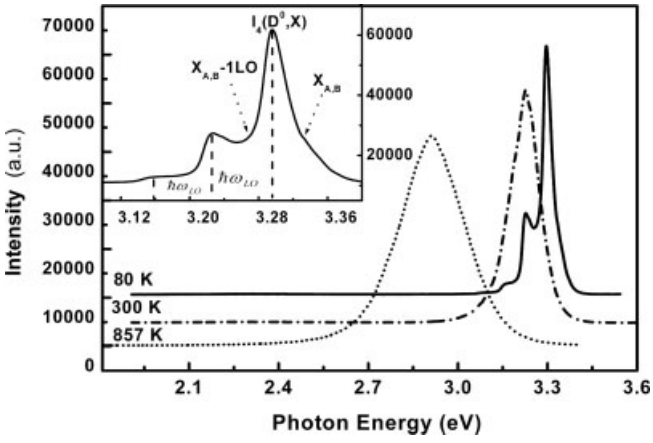

Figure 4. PL spectra of ZnO nanosheets measured at 80, 300, and 857 K. Inset indicates the detailed PL spectrum at 80 K along with the possible assignments.

80 K consists of several distinct peaks in the UV region. A zoom-in spectroscopic region around 3.261 eV, shown in an inset of Figure 4, illustrates that the strongest peak at

ADVANCED MATERIALS

3.298 eV, along with two phonon replicas on the lower energy side, is due to neutral-donor-bound exciton emission (I_4).[21,22] A shoulder on the higher-energy side of I_4 at ~3.340 eV with a possible phonon replica may be assigned to free exciton emission. On the other hand, the DL emission, commonly observed in ZnO nanostructures,[14–17] was found to be extremely weak (< 0.3 %) compared with the near band-edge emission. The PL spectrum at 300 K shows only one dominant and sharp exciton peak at 3.23 eV with no observable DL emission. Since DL emission is commonly due to structural defects, such as stacking faults and dislocations, as well as surface defects in many ZnO nanostructures, the absent DL emission in these nanosheets can only indicate that an undetectable concentration of structural defects is present. Hence, the ZnO nanosheets have a superior structural and optical quality to many of the ZnO nanostructures reported in the literature.[14–17]

Another noticeable feature is the remarkable photon emission even at 857 K. Emission at such high temperatures has not been reported from ZnO bulk and nanostructures. Based on the strength of the emission at 857 K, it is expected that significant emission would be detected at even higher temperatures, although it is beyond the capability of the temperature controller used here. As expected, the emission linewidth at 857 K is much broader than that of the room temperature PL peak. The peak position is red-shifted to ~2.91 eV. The intensity of the UV emission at room temperature is so strong that it had blurred the clearly visible edges of the sample when the excitation laser was turned off.

In order to study the origin of this emission peak, a temperature dependent measurement was conducted from 80 to 857 K, as shown in Figures 5a,b. Figure 5a is a set of temperatures-dependent PL spectra which are normalized against their peak height to illustrate the PL spectroscopic lineshape and linewidth. Figure 5b displays the integrated intensity of the nanosheet PL along with an optically thick ZnO nanocrystalline film as a function of sample temperature. Due to the fact that the PL peak position shows a systematic red-shift with a temperature increase, and it fits well with the emission energy of semiconductors described by the empirical formula:[23]

$$E(T) = E(0) - \frac{\alpha T^2}{T_0 + T} \quad (1)$$

where $E(0)$ is the optical bandgap maximum at 0 K and α and T_0 are fitting parameters, as illustrated in the insert of Figure 5a. Hence, it can be argued that the emission peak observed at 2.91 eV originates from an inter-band transition rather than those associated with defect-related emissions. Similar PL measurements on ZnO powders, ZnO films on Al_2O_3, and bulk ZnO at high temperature were also conducted and the results agreed well with the proposed argument. As demonstrated in Figure 5b, the emission arising from the inter-band transition of an optically thick nanocrystalline film clearly showed a decrease in PL intensity with temperature, and PL disappeared at ~500 K. However, the PL of the nanosheet exhibits a fairly strong intensity, even at 857 K. Although the physical mechanisms of why the ZnO nanosheets show such strong emission, even at 857 K, is not clearly understood and has not been reported in the past, attempts were made which may partially be attributed to the experimental observation. It is expected that the 2D nanosheet structure has a very low number of defects in and on the surface of the nanosheets. It is then formed into a high-quality single-layered quantum-well structure, i.e., air–ZnO nanosheet–air. As reported in the literature,[24–29] the

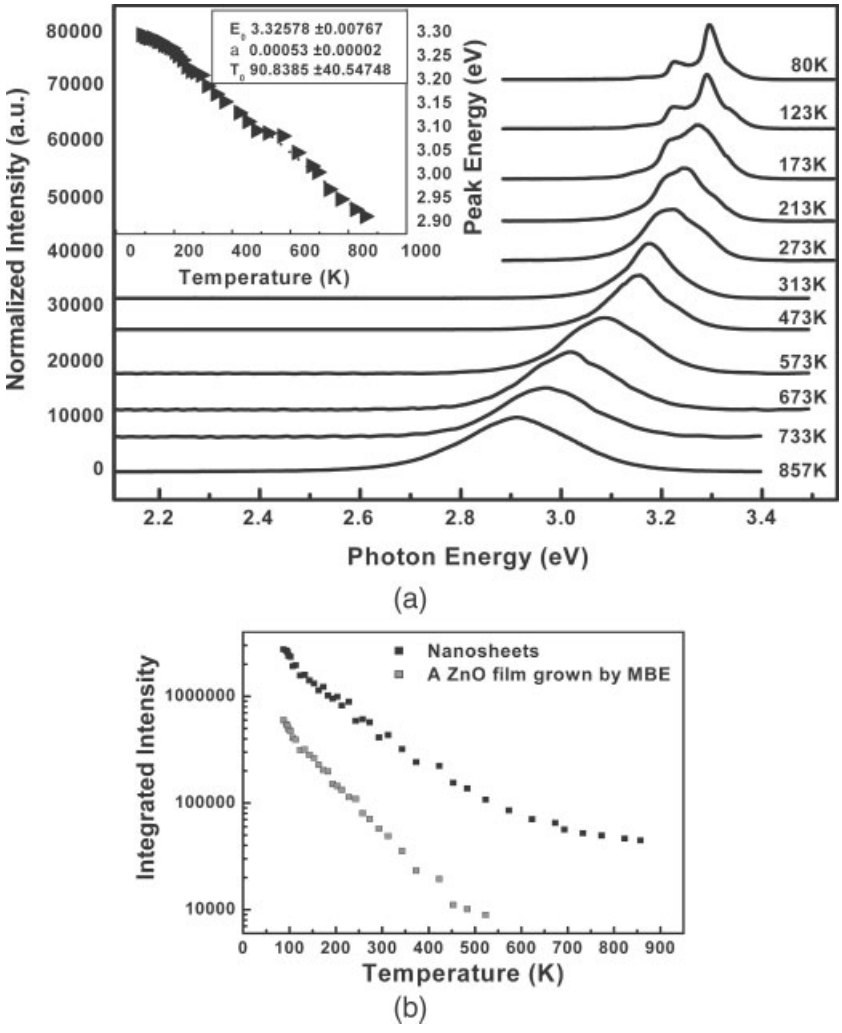

Figure 5. a) Temperature-dependent PL spectra in a temperature range of 80–857 K along with the peak position change with sample temperature and model fitting; b) temperature-dependent integrated PL intensity along with that of a high-quality and optically thick ZnO thin film grown by the MBE technique.

exciton binding energy in a quantum well has a strong dependence on quantum-well width, dielectric mismatch between the potential-barrier materials and the well, as well as the height of the potential barrier. The Rydberg number, R, can increase from its bulk value (or large well width) of $1R$, to a value of $4R$ at small width. In addition, the model calculation shows that there exists a critical well width at which the exciton-binding energy has its maximum value. The binding energy will decrease when the well width decreases. Therefore, it is quite possible that our observation of exciton-binding-energy enhancement is partly due to this mechanism. Unfortunately, we could not provide enough evidence to confirm whether or not this is the mechanism since we are unable to provide a high-resolution TEM analysis, which may show the presence of a much-narrowed well width. The observed high emission may be attributed to two physical processes: enhancement of oscillator strength and a microcavity effect. As reported by Gil and Kavokin,[30] a remarkable peculiarity of ZnO dots is that maximum enhancement of their oscillator strength is due to the Rashba–Gurgenishvili effect, and is given by a record value of about 13, which is a few times more than what one can expect in CdSe nanocrystals.[31] This is because the exciton Bohr radius in ZnO is two orders of magnitude less than the wavelength of light, λ, at the exciton-resonance frequency. This opens a way to observe the extremely strong exciton-light-coupling effects in ZnO quantum dots of about 30 nm in size. Hence, a similar effect should also exist in the case of a quantum-well structure. A microcavity and waveguiding effect is also possible in the nanosheet (air–nanosheet–air) since the nanosheet surface is very flat. The refractive-index mismatch between the ZnO (~2.1) and air (~1.0) can lead to attenuated total reflection occurring when the angle and the polarization of the excitation and emitted photons satisfy the boundary condition. A positive optical feedback could occur between the two surfaces, and would result in a significantly enhanced PL signal. At the same time, the low concentration of defects in the ZnO sheets will suppress the probabilities of non-radiative recombination and deep-level emission.

The growth of the catalyst-free nanosheets has many advantages. It excludes possible incorporation of catalytic impurities, which may occur during the condensation–precipitation process for the metal-catalyst-assisted vapor–liquid–solid (VLS) method. Furthermore, the micrometer-sized uniformly thin nanosheet structure has a large parallel planar surface free of defects. The ability to grow high quality ZnO nanosheets has potential applications in nanoscale photonic and electronic devices. The high-temperature luminescence from semiconductor nanomaterials is very attractive in many new device applications.

In summary, high-quality single crystalline ZnO nanosheets were grown by a vapor-transport method via thermal evaporation of Zn powder. Large quantities of uniform multilayer sheets with micrometer-sized lateral dimensions and a thickness of about 100 nm were obtained. An intense UV emission is observed with negligible defect-related visible emission at a temperature range of 80 to 857 K. The increase of the exciton binding energy may be attributed, in part, to the presence of the image charges well known to the quantum-well structure. However, the quantum-confinement effect alone is insufficient to explain the degree of the exciton-binding energy increase. The strong luminescence enhancement may in part result from: a) oscillator strength enhancement due to the quantum confinement; and b) a positive optical feedback in light cavities formed between the smooth interfaces of the two lateral sides of the sheets, which act as natural reflectors.

Experimental

The nanosheets were prepared by a vapor-transport process. Zn metal grains (purity 99.99 %) were used as a source material. Zn grains were first etched in a diluted 1 % HF solution and then washed thoroughly with deionized water. A clean quartz tube containing the Zn grains was carefully inserted into a furnace at room temperature. Pure N_2 (5 N) was used to purge the air-tight tube. The furnace was heated slowly to 600 °C. After 2 h baking, the N_2 was cut off and pure O_2 (5 N) was introduced into the furnace for another 2 h. After the furnace was naturally cooled to room temperature, a white product was formed inside the quartz tube. The material was collected and characterized using field-emission scanning electron microscopy (FESEM; S-4200), X-ray diffraction (XRD), and transmission electron microscopy (TEM). Raman spectra were measured with a JY HR800 microlaser Raman spectrometer with a back-scattering optical configuration. An argon ion laser at 488 nm was used as the excitation source. PL measurements were carried out with a micro-PL system at temperatures from 80 to 857 K. A He–Cd laser at 325 nm was used for PL excitation. A typical power of 5 mW was used for excitation.

Received: August 3, 2004
Final version: October 10, 2004

[1] Y. Arakawa, H. Sasaki, *Appl. Phys. Lett*. **1982**, *40*, 939.
[2] S. C. Jain, M. Willander, J. Narayan, R. Van Overstraeten, *J. Appl. Phys*. **2000**, *87*, 965.
[3] C. J. Lee, T. J. Lee, S. C. Lyu, Y. Zhang, H. Ruh, H. Lee, *Appl. Phys. Lett*. **2002**, *81*, 3648.
[4] M. H. Huang, S. Mao, H. Feick, H. Yan, Y. Wu, H. Kind, E. Weber, R. Russo, P. Yang, *Science* **2001**, *292*, 1897.
[5] Y. Dai, Y. Zhang, Q. K. Li, C. W. Nan, *Chem. Phys. Lett*. **2002**, *358*, 83.
[6] C. C. Tang, S. S. Fan, M. L. de la Chapelle, P. Li, *Chem. Phys. Lett*. **2001**, *333*, 12.
[7] M. H. Huang, Y. Wu, H. Feick, N. Tran, E. Weber, P. Yang, *Adv. Mater*. **2001**, *13*, 113.
[8] K. Park, J. S. Lee, M. Y. Sung, S. Kim, *Jpn. J. Appl. Phys., Part 1* **2002**, *41*, 7317.
[9] J. Zhang, W. Yu, L. Zhang, *Phys. Lett. A*. **2002**, *299*, 276.
[10] M. Shirai, K. Igeta, M. Arai, *J. Phys. Chem*. **2001**, *105*, 7211.
[11] N. Miyamoto, H. Yamamoto, R. Kaito, K. Kuroda, *Chem. Commun*. **2002**, 2378.
[12] T. Sasaki, M. Watanabe, *J. Phys. Chem*. **1997**, *101*, 10 159.
[13] Y. C. Zhu, Y. Bando, *Chem. Phys. Lett*. **2003**, *372*, 640.
[14] J. Q. Hu, Y. Bando, J. H. Zhan, Y. B. Li, T. Sekiguchi, *Appl. Phys. Lett*. **2003**, *83*, 4414.
[15] V. A. L. Roy, A. B. Djurisic, W. K. Chan, J. Gao, H. F. Lui, C. Surya, *Appl. Phys. Lett*. **2003**, *83*, 141.
[16] Y. J. Xing, Z. H. Xi, Z. Q. Xue, X. D. Zhang, J. H. Song, R. M. Wang, J. Xu, Y. Song, S. L. Zhang, D. P. Yu, *Appl. Phys. Lett*. **2003**, *83*, 1689.
[17] W. D. Yu, X. M. Li, X. D. Gao, *Appl. Phys. Lett*. **2003**, *84*, 2658.
[18] Y. C. Kong, D. P. Yu, B. Zhang, W. Q. Fang, S. Q. Feng, *Appl. Phys. Lett*. **2001**, *78*, 407.

ADVANCED MATERIALS

[19] a) M. H. Huang, S. Mao, H. Feick, H. Yan, Y. Wu, H. Kind, E. Weber, R. Russo, P. Yang, *Science* **2001**, *292*, 1897. b) P. Yang, C. M. Lieber, *J. Mater. Res.* **1997**, *12*, 2981.
[20] T. C. Damen, S. P. S. Porto, B. Tell, *Phys. Rev.* **1966**, *142*, 570.
[21] S. J. Chen, Y. C. Liu, Y. M. Lu, J. Y. Zhang, D. Z. Shen, X. W. Fan, *J. Phys.: Condens. Matter* **2003**, *15*, 1975.
[22] F. A. Kroger, H. J. Vink, *J. Chem. Phys.* **1954**, *22*, 250.
[23] Y. P. Varshi, *Physics* **1967**, *34*, 149.
[24] R. Zheng, M. Matsuura, *Phys. Rev. B.* **1998**, *58*, 10 796.
[25] B. Gerlach, J. Wusthoff, M. O. Dzero, M. A. Smondyrev, *Phys. Rev. B.* **1998**, *58*, 10 568.
[26] A. V. Filinov, C. Riva, F. M. Peeters, Y. E. Lozovik, M. Bonitz, *Phys. Rev. B.* **2004**, *70*, 35 323.
[27] T. Someya, H. Akiyama, H. Sakaki, *Phys. Rev. Lett.* **1996**, *76*, 2965.
[28] U. Woggon, K. Hild, F. Gindele, W. Langbein, *Phys. Rev. B.* **2000**, *61*, 12 632.
[29] S. de-Leon, B. Laikhtman, *Phys. Rev. B.* **2000**, *61*, 2874.
[30] B. Gil, A. V. Kavokin, *Appl. Phys. Lett.* **2002**, *81*, 748.
[31] D. J. Norris, A. L. Efros, M. Rosen, M. G. Bawendi, *Phys. Rev. B.* **1996**, *53*, 16 347.

Fully Transparent ZnO Thin-Film Transistor Produced at Room Temperature**

By *Elvira M. C. Fortunato*,* *Pedro M. C. Barquinha*, *Ana C. M. B. G. Pimentel*, *Alexandra M. F. Gonçalves*, *António J. S. Marques*, *Luís M. N. Pereira*, and *Rodrigo F. P. Martins*

Functional oxide materials currently represent a key challenge as well as a promising powerful tool for both fundamental understanding and technological development of the next generation of transparent electronics, such as field-effect transistors.[1] Here, we report a fully transparent ZnO thin-film transistor (ZnO-TFT) with a transmittance above 80 % in the visible part of the spectrum, including the glass substrate, fabricated by radiofrequency (rf) magnetron sputtering at room temperature, with a bottom gate configuration. The ZnO-TFT operates in the enhancement mode, exhibiting a high saturation mobility of about 20 $cm^2 V^{-1} s^{-1}$, a threshold voltage of 21 V, a gate-voltage swing of 1.24 V $decade^{-1}$, and an on/off ratio of 2×10^5. Besides this, the off resistance is on the order of 20 MΩ and the on resistance is on the order of 45 kΩ. The combination of transparency, high mobility, and room-temperature processing makes the ZnO-TFT a very promising low-cost optoelectronic device for the next generation of invisible and flexible electronics, such as switching for addressing active matrices based on organic light-emitting diodes (OLEDs).

Thin-film transistors made with amorphous silicon and polysilicon have become the key components of the electronic flat-panel-display industry over the last ten years, just as silicon chips were earlier called the staple of the electronic computer revolution.[2] Nevertheless, thin-film transistors based on amorphous silicon technology present some limitations, such as light sensitivity and light degradation accompanied by a low mobility ($\mu \leq 2$ $cm^2 V^{-1} s^{-1}$). On the other hand, in spite of exhibiting a high mobility ($50\ cm^2 V^{-1} s^{-1} \leq \mu \leq 500\ cm^2 V^{-1} s^{-1}$), the opacity of polysilicon TFTs limits the aperture ratio for active matrix arrays; this is highly important, for instance, when OLEDs have to be addressed. Also, if flexible substrates based on polymers are intended to be used, the processing temperature is quite a limiting factor.

One possible way to overcome such problems is the utilization of efficient and reliable oxide-based thin-film transistors. Transparent-oxide-semiconductor-based transistors have recently been proposed, using intrinsic zinc oxide (ZnO) as an active channel.[3–8] One of the main advantages exhibited by these transistors lies in the magnitude of the electron-channel mobility, leading to higher drive currents and faster device operating speeds. The mobility reported in the literature ranges from 0.2–7 $cm^2 V^{-1} s^{-1}$, with an on/off current ratio from 10^5–10^7, and a threshold voltage (V_{TH}) between –1 V and 15 V. Until now, most ZnO channel layers have been deposited using substrate heating or subjected to post-thermal annealing, mainly in order to increase the crystallinity of the ZnO layer and thus the mobility in the film.

The purpose of this work is to demonstrate the possibility of fabricating high-mobility ZnO thin-film transistors at room temperature by rf magnetron sputtering with improved performances and highly compatible with the fabrication technologies used for flexible electronics. By doing so, we overcome processing-temperature limitations, making it possible for the devices to be used in a wide range of applications where the mobility is no longer a limitation, such as for use in so-called fast and invisible electronics.

Figure 1 shows the dependence of the electrical resistivity (ρ) and the average optical transmittance in the visible spectra (between 400–700 nm) as a function of rf power density (P). The highest resistivity ($\approx 10^8$ Ω cm) was obtained for $P = 5$ W cm^{-2}. For $P \sim 5$ W cm^{-2}, the films were close to being stoichiometric with few structural defects and a consequently higher resistivity. As we decreased or increased the rf power density from 5 W cm^{-2}, a deviation from stoichiometry was obtained, accompanied by a decrease in electrical resistivity due to a lower carrier concentration and/or electron mobility. This was also confirmed by a decrease in the optical transmittance, especially for rf power densities lower than 5 W cm^{-2}.

[*] Prof. E. M. C. Fortunato, P. M. C. Barquinha, A. C. M. B. G. Pimentel, A. M. F. Gonçalves, A. J. S. Marques, L. M. N. Pereira, Prof. R. F. P. Martins
Department of Materials Science/CENIMAT
Faculty of Sciences and Technology
New University of Lisbon and CEMOP-UNINOVA
Campus da Caparica
P-2829-516 Caparica (Portugal)
E-mail: elvira.fortunato@fct.unl.pt

[**] The authors thank Planar Systems, Inc., Espoo, Finland, for supplying the ITO/ATO glass substrates. This work was partially financed by the Portuguese Science Foundation (FCT-MCIES) through the pluriannual contract of CENIMAT.

  DOI: 10.1002/adma.200400368